IRAQI JOURNAL OF MATERIALS
Volume (1) Issue (1) January-March 2022, pp. 7-14

Structural Analysis of Surface Modified Titanium Dioxide Nanostructures Synthesized by Reactive Sputtering

Esraa A. Al-Oubidy, Firas J. Kadhim

Department of Physics, College of Science, University of Baghdad, Baghdad, IRAQ

Abstract
In this study, the structural characteristics of the surface modified-titanium dioxide nanostructured thin films prepared by dc reactive sputtering technique were determined and compared. The modifications were carried out by doping of titanium dioxide nanostructures with metal (Ag) and non-metal (N) dopants. The structural characteristics were introduced by the scanning electron microscopy and energy-dispersive x-ray spectroscopy. Surface modifications are highly-required for the employment of titanium dioxide nanostructures in efficient photocatalyst applications.

Keywords: Titanium dioxide; Nanostructures; Surface modification; Reactive sputtering
Received: 2 May 2021; **Revised:** 9 September; **Accepted:** 16 September 2021; **Published:** 1 January 2022

1. Introduction

1.2 Semiconductor Photocatalyst

The primary criteria for an efficient semiconductor photocatalyst is that the redox potential of the charge couple, i.e., e^-/h^+, lies within the band gap domain of the photocatalyst. The energy level at the bottom of conduction band determines the reducing ability of photoelectrons, while the energy level at the top of valence band determines the oxidizing ability of photogenerated holes [1]. The internal energy scale is given on the left for comparison to normal hydrogen electrode (NHE). The positions are derived from the flat band potentials in a contact solution of aqueous electrolyte at pH = 1. The pH of the electrolyte solution influences the band edge positions of the various semiconductors compared to the redox potentials for the adsorbate [2].

A semiconductor photocatalysts should also be easy to produce and use, cost effective, photostable, nonhazardous for humans and the environment, effectively activated by solar light and able to catalyze the reaction effectively [3]. Most of the reported photocatalysts possess limitations, e.g., GaAs, PbS, and CdS are not sufficiently stable for catalysis in aqueous media as they readily undergo photocorrosion and are also toxic [4]. ZnO is unstable because it readily dissolves in water to yield Zn $(OH)_2$ on the ZnO particle surface, which inactivates the catalyst over time [5]. Fe_2O_3, SnO_2, and WO_3 possess a conduction band edge at an energy level below the reversible hydrogen potential, thus systems using these materials require application of an external electrical bias to complete the water splitting reaction and achieve hydrogen evolution at the cathode [6,7].

TiO_2 is close to be an ideal photocatalyst and the benchmark for photocatalysis performance. TiO_2 is cheap, photostable in solution and nontoxic. Its holes are strongly oxidizing and redox selective. For these reasons, several novel heterogeneous photocatalytic reactions have been reported at the interface of illuminated TiO_2 photocatalyst, and TiO_2-based photocatalysis has been researched exhaustively for environmental cleanup applications. The single drawback is that it does not absorb visible light [8]. To overcome this problem, several methods including dye sensitization, doping, coupling and capping of TiO_2 are proposed.

Titanium dioxide (TiO_2) -also known as titania- is a white inorganic solid substance that is thermally stable, insoluble in water, chemically inert, non-flammable and not classified as a hazardous substance according to the United Nations (UN) Globally Harmonized System of Classification and Labeling of Chemicals [9]. TiO_2 is widely used in industrial applications such as catalyst support, dye-sensitized photoelectrochemical solar cells, in consumer goods (paints, coatings, printing inks, cosmetics, ceramics, textiles, etc.) and also in the pharmaceuticals sector. In addition, TiO_2 continues to receive much attention from researchers for its application as a photocatalyst [10]. TiO_2 belongs to the family of transition metal oxide and exists in nature in one of the three crystalline forms; rutile, anatase and

brookite. In addition to these common polymorphs [11]. Among the three crystalline TiO_2 phases, anatase and rutile are the most researched crystalline forms with respect to photocatalysis because they can be prepared easily in pure form by synthesizing from titanium containing compounds. Relatively little is known about the brookite form because it occurs quite rarely, is unstable and difficult to prepare without the presence of anatase and rutile; that is why it is not often used for experimental investigation [12].

Rutile is the most common mineral form of TiO_2 in nature. The rutile structure is not compact and its unit cell is tetragonal: one axis is 30% shorter than the two others (a = 4.593 Å, c = 2.959 Å). The structure is constituted by much distorted octahedral TiO_6, with oxygen ions shared with other adjacent Ti ions [13]. Every Ti ion is an octahedral surrounded by six O ions, and every O ion is surrounded by three Ti ions at the edges of an equilateral triangle. It can be envisaged as a body center cubic lattice of Ti ions that is considerably distorted [14]. The crystallites can be present in nature as black or reddish and also transparent when completely without impurities. The color can also be orange if the mineral is in very thin needle form [15].

Anatase, also improperly called octahedrite, presents a tetragonal bipyramidal symmetry, with a form similar to an elongated octahedron (a=3.785Å, c=9.514Å). The structure is based on a polyhedral chain of TiO_6. The difference from rutile is that anatase presents a more distorted structure, where every polyhedron shares 4 edges with the adjacent one. In particular, the tetragonal elementary cell contains 4 units, instead of 2, and the cell sides are a=3.785Å and c=9.514Å. The anatase crystals are really small, the natural color ranges from blue sapphire to yellow-brown [16,17]. These differences in lattice structures cause different mass densities and electronic band structures for the two main TiO_2 polymorphs. In particular, TiO_2 is characterized by an allowed and indirect band gap, which is equal to 3.2 and 3.0 eV, respectively, for the anatase and rutile phases [18]. This polymorph is metastable: out of a restricted pressure and temperature interval it is converted into the two other phases.

Anatase shows better photocatalytic activity due to its higher surface area and porosity (which provide a higher number of catalytic sites), greater number of hydroxyl groups, and optimum band gap and exhibits lower rates of excited electron-hole pair recombination. Moreover, the electron transfer from the conduction band to O_2 is energetically easier at the anatase surface because conduction band in anatase has higher energy than that of rutile phase [19,20].

A requirement for the initiation of photocatalytic reaction is the absorption of light with energy equal to or higher than the bang gap of the photocatalytic material. The band gap width is approximately 3.2 eV (λ = 388 nm) for anatase, 3.0 eV (λ= 414 nm) for rutile and 3.2 eV (λ = 388 nm) for brookite [21]. Among the three polymorphs of TiO_2, anatase has proved to be more effective than brookite and/or rutile in the photocatalytic applications [22]. When this occurs, the excited electrons (e^-) can move from the valence band (composed of the 2p orbitals of oxygen) to the conduction band (3d orbitals of titanium), with the concurrent generation of the holes (h^+) in the valence band [23,24]. During the photocatalytic reaction, two major events occur simultaneously: reduction of an electron acceptor, e.g., oxygen, by photoexcited electrons and oxidation of electron donor, e.g., water present, by photogenerated holes. The resulting radicals, like $O_2^{\cdot-}$ and $OH^{\cdot}$, can then further react with the target compounds (impurities, pollutants).

One of the most active fields of research in heterogeneous photocatalysis using semiconductor particles is the development of a system capable of using natural sunlight to degrade a large number of organic and inorganic contaminants in wastewater [25-27]. The overall photocatalytic activity of a particular semiconductor system for the stated purpose is measured by several factors including the stability of the semiconductor under illumination, the efficiency of the photocatalytic process, the selectivity of the products, and the wavelength range response. For example, small band-gap semiconductors such as CdS are capable of receiving excitation in the visible region of the solar spectrum, but are usually unstable and photodegrade with time [28].

Titanium dioxide is a quite stable photocatalyst, but since the band gap is large (for example E_g=3.2eV to Anatase phase) it is only active in the ultraviolet region which is <10% of the overall solar intensity [29].

The limitations of a particular semiconductor as a photocatalyst for a particular use can be surmounted by modifying the surface of the semiconductor. To date, two benefits of modifications to photocatalytic semiconductor systems: (1) inhibiting recombination by increasing the charge separation and therefore the efficiency of the photocatalytic process; (2) increasing the wavelength response range (i.e. excitation of wide band gap semiconductors by visible light).

Modification of TiO_2 can lead to desired photocatalytic activity under visible light (400-700 nm) to obtain more effective photocatalysts with greater activity under UV-light irradiation or to obtain photocatalysts which may be active also under visible light irradiation [30].

 ISSN (print) 2958-8960 (online) xxxx-xxxx Printed in IRAQ

In photocatalysis, the addition of metals (such as Ag, Pd, Cr, Fe, Cu, Pt, etc.) to a semiconductor can change the photocatalytic process by changing the semiconductor surface properties, the contact between a semiconductor and metal generally involves a redistribution of electric charges and the transfer of mobile charge carriers between the semiconductor and metal doped, or the trapping of charge carriers at surface states at the interface, produces a space charge layer. The electrons will migrate from the semiconductor to the metal, because the metal has a higher work function than the semiconductor [31].

The surface of the metal acquires an excess negative charge while the semiconductor exhibits an excess positive charge as a result of electron migration away from the barrier region. The barrier formed at the metal-semiconductor interface is called the Schottky barrier, as shown in Fig. (1) [32].

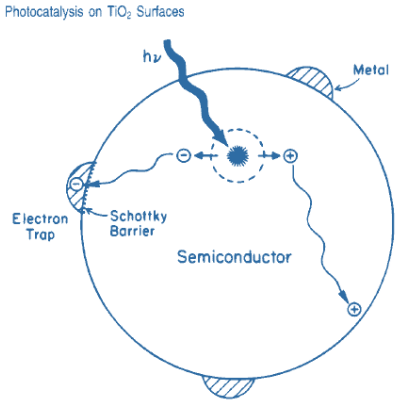

Fig. (1) Metal-modified semiconductor photocatalyst particle

If the depletion of the majority charge carriers extends far into the semiconductor, the Fermi level can decrease below the level of the conduction band, as shown in Fig. (2a) [33]. After the electron migrates to the metal, it becomes trapped and electron-hole recombination is suppressed. In addition, the decrease in electron density within the semiconductor leads to an increase in the hydroxyl group. This in turn affects the photocatalytic process on the semiconductor surface [61].

Most non-metal elements such as B, C, N and F have also been used as dopants in TiO_2 photocatalysts [2–6]. Nitrogen-doped TiO_2 is by far the most intensively studied system among the other non-metal doped materials. The N-atoms can be easily introduced to TiO_2 lattice due to their comparable atomic size to oxygen, small ionization energy and high stability [9]. TiO_2 doped with non-metal (N-atoms) at oxygen sites serve as charge (electrons and holes) trapping sites to reduce electron hole recombination rate .and allow absorption into the visible region due to the introduction of dopant impurity level in TiO_2 band gap. Thus the photocatalytic performance in enhanced compared to undoped photocatalyst [7,21].

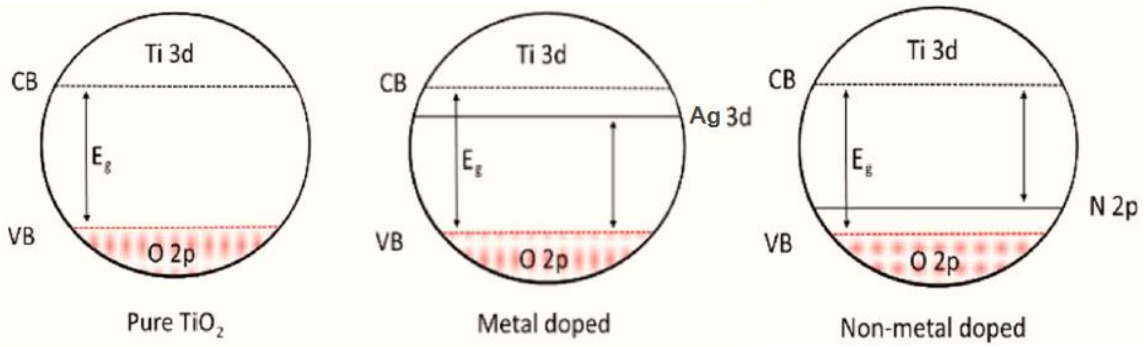

Fig. (2) Band gap narrowing of TiO_2 due to metal dopants (Ag) and non-metal dopants (N)

In TiO_2, the 3d orbitals of Ti govern the conduction band (CB) and O 2p orbitals dominate the valance band (VB). Non-metal doping usually produces impurity levels in the forbidden gap or resonate with the bottom of the CB while anion doping mostly modifies the valance band due to different p orbitals in relation to the O 2p orbitals [2]. The doping process has some advantages. First, reduction in the band gap (either by increasing the top of valance band or lowering the bottom of conduction band) or to

introduce intra-band gap states for the goal to achieve more visible light absorption (Fig. 2b). Second, trapping of the photogenerated electrons and holes leads to a decrease in the recombination rate.

2. Experimental Part

Titanium (Ti) sheet of 99.9% purity, 7.5 cm diameter and 0.5 mm thickness was used as sputtering target to prepare titanium dioxide (TiO_2). The films were deposited on transparent substrates made of borosilicate glass. Before using these substrates in sputtering experiments, they were first cleaned with ethanol to remove any oil layers or residuals may exist on their surfaces, washed with distilled water to remove ethanol, and then dried completely before being kept in clean case or placed inside vacuum chamber.

The gas mixture is allowed to flow from the gas mixing unit into the chamber throughout a needle valve to keep the pressure of gas mixture constant inside the deposition chamber. In order to prepare un-doped TiO_2 films, only oxygen was used as a reactive gas, while the nitrogen was added to the gas mixture to prepare TiO_2 film doped with nitrogen. The pressures of oxygen and nitrogen gases should to be relatively low to avoid the situation of target poisoning.

Many parameters could be used to control the operation and sputtering processes in this work. These parameters were classified into two groups; constant and variable. The constant parameters include discharge voltage, discharge current and base pressure in the chamber. The variable parameters include the inter-electrode distance, which could be adjusted from 0 to 8 cm, and deposition time. In addition, the mixing ratio of process gas (Ar) and reactive gases (O_2 and/or N_2) plays an important role in finalizing the deposition process and appearance of thin films, as can be seen in Fig. (2). The gas mixing ratio ($Ar:O_2$ or $Ar:O_2:N_2$) was varied over a wide range but only the ratios presented in table (1) were considered to prepare the optimum samples; single-phase and mixed-phase, undoped and doped TiO_2 films.

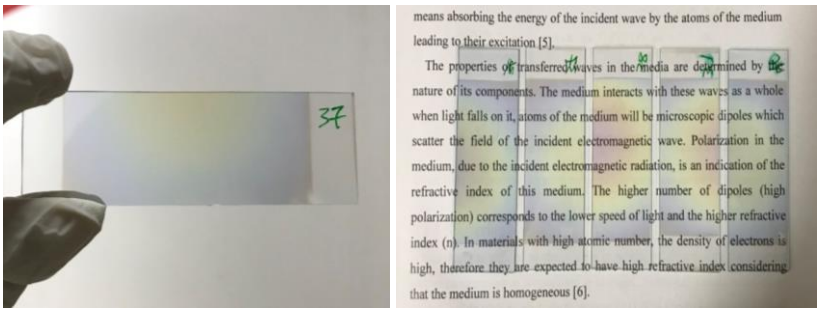

Fig. (2) Photographs of undoped (left) and N-doped (right) TiO_2 films

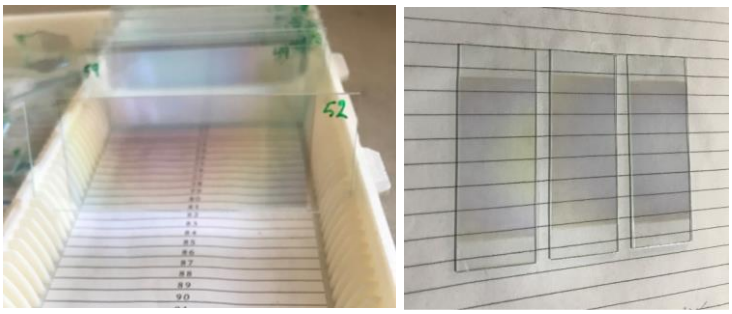

Fig. (3) Photographs of some Ag-doped TiO_2 films prepared in this work

In order to synthesize the Ag-doped TiO_2 thin films, the co-sputtering configuration of 99.9% purity titanium (Ti) sheet and 99.99% purity silver (Ag) was used. The two sheets were mounted with some geometrical arrangement. The geometrical arrangement shown above was proposed according to a numerical treatment carried out to determine the dimensions of both sheets with respect to each other to achieve the required doping process. This geometrical arrangement was considered as soon as the formation of Ag-doped TiO_2 thin films, it can see the final prepared films in Fig. (3), was confirmed by the x-ray diffraction (XRD) pattern. However, the $Ar:O_2$ mixing ratio, presented in table (1), play very important roles in determining the characteristics of the Ag-doped TiO_2 samples prepared using such geometrical arrangement.

 ISSN (print) 2958-8960 (online) xxxx-xxxx Printed in IRAQ

Table (1) Summary of the gas mixtures sued to prepare optimum TiO_2 samples in this work

Prepared samples		Ar ratio (%)	O_2 ratio (%)	N_2 ratio (%)	Phase
Undoped TiO_2	Without heat sink	50	50	-	Mixed-phase (anatase/ rutile)
		67	33	-	
		80	20	-	
		83	17	-	
		87	13	-	
	With heat sink	50	50	-	Single-phase (anatase)
		67	33	-	
		80	20	-	
		83	17	-	
		87	13	-	
N-doped TiO_2	With heat sink	40	40	20	Single-phase (anatase)
		60	30	10	
		76	19	5	
Ag-doped TiO_2	With heat sink	50	50	-	Single-phase (anatase)
		67	33	-	
		80	20	-	

Different measurements were carried out on the prepared un-doped and doped titanium dioxide samples in order to characterize, classify and optimize them towards the main goal of this work. They include thickness measurements, x-ray diffraction (XRD) pattern, atomic force microscopy (AFM), scanning electron microscopy (SEM), and energy-dispersive x-ray spectroscopy (EDX).

The XRD is one of the most powerful techniques for qualitative analysis of crystalline compounds. In this study, the crystalline structure of prepared thin films was examined by Bruker D2 PHASER XRD technique under the condition of power diffraction system with Cu-Kα x-ray tube (λ = 1.54056 Å). The x-ray scans were recorded in the range of diffraction angle (2θ) from 20° to 80°. The overall structure of thin film includes lattice constants and grain size identification of unknown materials. The weight fraction of the rutile phase in mixed-phase (rutile+anatase) TiO_2 can be determined from XRD peak by the following equation [3]:

$$f = \frac{1}{1+1.26\frac{I_R}{I_A}} \quad (1)$$

where *f* is the weight fraction of rutile in mixed-phase sample, and (I_R/I_A) is the ratio of intensity of rutile to the intensity of anatase as determined from the x-ray pattern

The atomic force microscopy (AFM) was performed using Angstrom AA3000 instrument on the samples prepared at the optimum conditions in order to study their nanoscale surface topography as well as to introduce the effects of some operation conditions on the surface topography of the prepared samples. The scanning electron microscopy (SEM) was performed on the prepared samples using a PHENOM PURE 30000X instrument. The samples prepared at the optimum conditions were measured in order to confirm the formation of nanostructures as well as introduce the effects of some operation conditions on the fine structures of the prepared samples. The energy-dispersive x-ray (EDX) spectroscopy was carried out using a PHENOM PURE 30000X instrument to identify the elemental composition of the final sample. In this technique, the sample is bombarded by an energetic electron beam and the collisions have a high probability to knock out the inner-shell electrons of the constituent atoms. The created vacancy is rapidly filled by an electron from higher lying shell and this transition results in the secondary emission of fluorescence x-rays. The wavelengths depend on the energy difference between the two shells involved in the electronic transition, so that the energy of emitted x-rays is uniquely characteristic of particular element. In other words, the elemental composition is directly determined by measuring the energy of emitted x-ray [13].

Based on EDX results, the SEM/EDX mapping, which is a valuable tool to indicate the quality of the synthesized structures. The electron beam is scanned pixel by pixel across a selected area of interest. Generally, the brighter the color appears, the higher is the concentration of the specific element [5]. The spatial resolution in the SEM EDX mapping is related to the interaction volume of primary electron beam and consequently x-ray generation volume [16].

3. Results and Discussion

Surface profile and particle size for the prepared thin films – those considered optimum to fabricate nanophotocatalysts – were determined by scanning electron microscopy (SEM). The SEM images of undoped and doped TiO_2 films are shown in Fig. (7). The first feature can be seen in these images is the homogeneity of particle distributions, which is one of the most important advantages of DC magnetron sputtering technique used for synthesis of nanostructures. Another important feature can be seen is the absence of aggregation over the scanned sample. This may be attributed to the heat sink mechanism employed to prevent anatase phase from converting into rutile in the TiO_2 samples. However, the inter-space between nanoparticles in the anatase samples was apparently larger than that in mixed-phase TiO_2 samples. This can be interpreted as follows: in single phase structure, such as anatase TiO_2 sample prepared in this work, it is very difficult to produce intertwined nanostructures as an anisotropic growth results from the different 9 crystal planes existing in the prepared sample. This suggests a surface transformation from flat to quasi continuous high-index facets [19]. On the other hand, in a multiphase structure, such as mixed-phase TiO_2 samples prepared in this work, the 13 crystal planes can form intertwined facets and hence the inter-space between nanoparticles may be minimized and the nano-surface show much more flatness than in the single-phase situation [20].

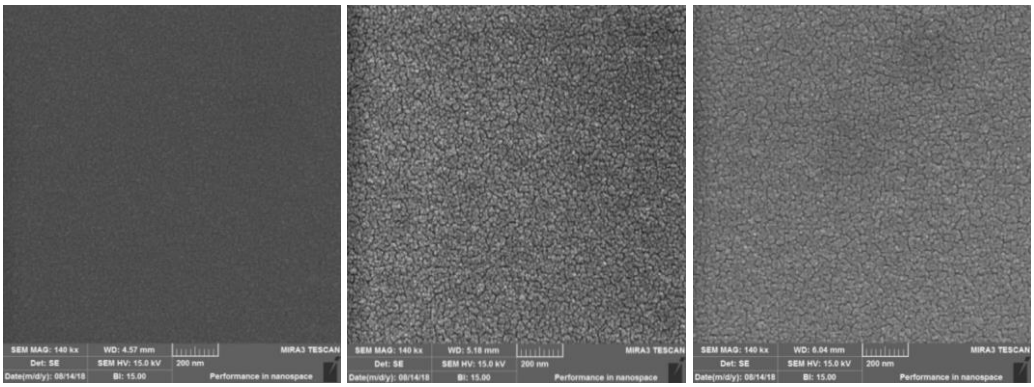

Fig. (7) SEM images of undoped mixed-phase of TiO_2 (left), undoped anatase-phase of TiO_2 (center), and N-doped of TiO_2 (right)

In the N-doped TiO_2 samples, the inter-space between nanoparticles is comparable to that in single-phase samples, which is an inevitable result to the presence of gas species (N) within the structure [2]. However, the N-doped TiO_2 samples exhibited higher roughness (~65nm) than mixed-phase samples (~37nm). In the Ag-doped TiO_2 sample (Fig. 8), the inter-space between nanoparticles is reasonably large when compared to other samples. This may be attributed to the tendency of Ag atoms to bond with O atoms to form silver oxides and hence large clusters may be grown. Otherwise, Ag atoms may replace Ti atoms in the TiO_2 lattice as dopants and hence the particle size may not be increase.

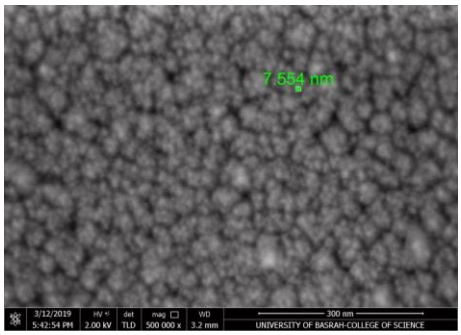

Fig. (8) SEM images of Ag-doped of TiO_2

According to the analysis software used to determine the particle size in the nanostructures prepared in this work, the particle size of TiO_2 nanoparticles was determined to be about 25 nm and 20 nm for mixed-phase and single-phase undoped TiO_2 samples, respectively, while the particle size for N-doped and Ag-doped TiO_2 nanostructures is about 15 nm and 8 nm, respectively.

The energy-dispersive x-ray (EDX) spectra for the prepared samples were recorded and analyzed as shown in figures (9), (10) and (11). The summary of elemental compositions in the final samples is presented in the tables below these figures. With the existence of Ti and O in the final sample, the weight ratio of Ti:O was found to be 75.4:24.6 and 73.7:26.3 for mixed-phase and single-phase undoped TiO_2 samples, respectively. For N-doped of TiO_2 sample, the weight ratio of Ti:O was 27.7:72.3. These results confirmed the stoichiometry of the TiO_2 molecules as they completely agree with the chemical bonding configuration of such compound. In case of undoped TiO_2 samples, no impurities were detected as supported by the atomic integration of Ti and O elements. This feature is highly preferred for studies concerned to the concepts of physical and chemical characteristics and processes.

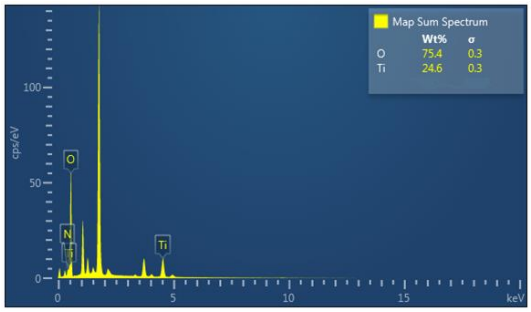

Fig. (9) EDX results of undoped mixed-phase of TiO_2

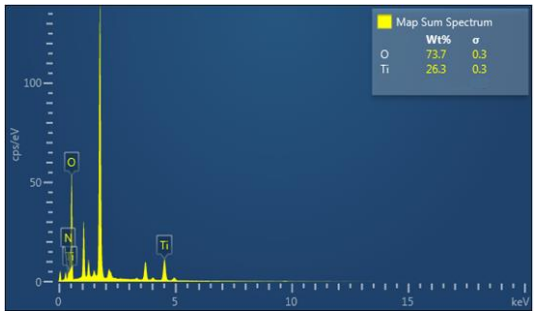

Fig. (10) EDX results of undoped anatase phase of TiO_2

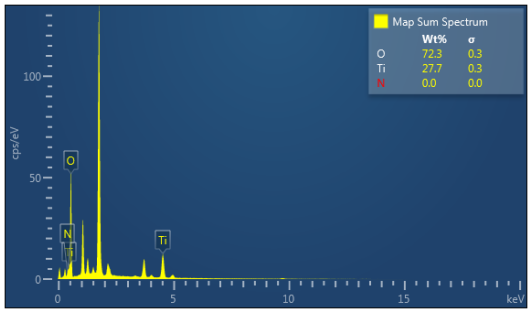

Fig. (11) EDX results of N-doped of TiO_2

4. Conclusion

In this study, the structural characteristics of the surface modified-titanium dioxide nanostructured thin films prepared by dc reactive sputtering technique were determined and compared. The modifications were carried out by doping of titanium dioxide nanostructures with metal (Ag) and non-metal (N) dopants. The structural characteristics were introduced by the scanning electron microscopy and energy-dispersive x-ray spectroscopy. Surface modifications are highly-required for the employment of titanium dioxide nanostructures in efficient photocatalyst applications.

References

[1] A. Monsi, M.R. Foroughi and M.R. Monshi, “Modified Scherrer Equation to Estimate More Accurately Nano-Crystallite Size Using XRD”, *World J. Nano Sci. Eng.*, 2 (2012) 154-160.

 ISSN (print) 2958-8960 (online) xxxx-xxxx Printed in IRAQ

[2] A. Zachariah et al., "Synergistic Effect in Photocatalysis As Observed for Mixed-Phase Nanocrystalline Titania Processed via Sol-Gel Solvent Mixing and Calcination", *J. Phys. Chem. C*, 112 (2008) 11345-11356.
[3] E.A. Al-Oubidy and F.J. Al-Maliki, "Effect of Gas Mixing Ratio on Energy Band Gap of Mixed-Phase Titanium Dioxide Nanostructures Prepared by Reactive Magnetron Sputtering Technique", *Iraqi J. Appl. Phys.*, 14(4) (2018) 19-23.
[4] A.L. Linsebigler, G. Lu, and J.T. Yates, "Photocatalysis on TiO_2 Surfaces: Principles, Mechanisms, and Selected Results", *Chem. Rev.*, 95(3) (1995) 735-758.
[5] C. Byrne et al., "New approach of modifying the anatase to rutile transition temperature in TiO_2 photocatalysts", *RSC Adv.*, 97(6) (2016) 95232-95238.
[6] F.J. Al-Maliki and E.A. Al-Oubidy, "Effect of gas mixing ratio on structural characteristics of titanium dioxide nanostructures synthesized by DC reactive magnetron sputtering", *Physica B: Cond. Matter*, 555 (2019) 18-20
[7] C.S. Kim et al., "Solvothermal synthesis of nanocrystalline TiO_2 in toluene with surfactant", *J. Cryst. Growth*, 257 (2003) 309-315.
[8] E.A. Al-Oubidy and F.J. Al-Maliki, "Photocatalytic activity of anatase titanium dioxide nanostructures prepared by reactive magnetron sputtering technique", *Opt. Quantum Electron.*, 51(1-2) (2019) 23.
[9] F. Amano et al., "Photocatalytic activity of octahedral single-crystalline mesoparticles of anatase titanium(IV) oxide", *Chem. Commun.*, 17 (2009) 2311-2313.
[10] F.J. Al-Maliki and N.H. Al-Lamey, "Synthesis of Tb-Doped Titanium Dioxide Nanostructures by Sol-Gel Method for Environmental Photocatalysis Applications" *J. Sol-Gel Sci. Technol.*, 81(1) (2017) 276-283.
[11] H.A. Alhadrami et al., "Antibacterial Applications of Anatase TiO_2 Nanoparticle", *Am. J. Nanomater.*, 5(1) (2017) 31-42.
[12] I. Karabay et al., "Structural and Optical Characterization of TiO_2 Thin Films Prepared by Sol–Gel Process", *Acta Physica Polonica A*, 121(1) (2012) 265-267.
[13] J. Biener et al., "Surface Chemistry in Nanoscale Materials", *Materials*, 2 (2009) 2404-2428.
[14] J.O. Carneiro et al., **"Self-cleaning smart nanocoatings, Nanocoatings and Ultra-Thin Films: Technologies and Applications"**, Woodhead Publishing Series in Metals and Surface Engineering, 2011, Pages 397-413.
[15] JCPDS card no. 3-0380 (TiO_2), **"Standard X-ray Diffraction Powder Patterns"**, US Department of Commerce, National Bureau of Standards, Vol. 25, Sec. 3, p. 57.
[16] K. Eufinger, "Effect of deposition conditions and doping on the structure, optical properties and photocatalytic activity of d.c. magnetron sputtered TiO_2 thin films", Ph.D. thesis, Ghent University, Belgium (2007).
[17] F.J. Al-Maliki, O.A. Hammadi and E.A. Al-Oubidy, "Optimization of Rutile/Anatase Ratio in Titanium Dioxide Nanostructures prepared by DC Magnetron Sputtering Technique", *Iraqi J. Sci.*, 60(special issue) (2019) 91-98.
[18] K. Zakrzewska and M. Radecka, "TiO_2-Based Nanomaterials for Gas Sensing - Influence of Anatase and Rutile Contributions", *Nanoscale Res. Lett.*, 12 (2017) 89-96.
[19] M. Aravind, M. Amalanathan and M. Sony Michael Mary, "Synthesis of TiO_2 nanoparticles by chemical and green synthesis methods and their multifaceted properties", *SpringerNature Appl. Sci.*, 3 (2021) 409.
[20] M. Sundrarajan and S. Gowri, "Green synthesis of titanium dioxide nanoparticles by nyctanthes arbor-tristis leaves extract", *Chalcog. Lett.*, 8(8) (2011) 447-451.
[21] F.J. Al-Maliki, O.A. Hammadi, B.T. Chiad and E.A. Al-Oubidy, "Enhanced photocatalytic activity of Ag-doped TiO_2 nanoparticles synthesized by DC Reactive Magnetron Co-Sputtering Technique", *Opt. Quantum Electron.*, 52 (2020) 188.
[22] N.T. Nolan, "Sol-Gel Synthesis and Characterization of Novel Metal Oxide Nano-materials for Photocatalytic Applications", Ph.D. thesis, Dublin Institute of Technology, Ireland (2010).
[23] O. Carp, C.L. Huisman and A. Reller, "Photoinduced reactivity of titanium dioxide", *Prog. Sol. Stat. Chem.*, 32 (2004) 33-117.
[24] O.A. Hammadi, "Production of Nanopowders from Physical Vapor Deposited Films on Nonmetallic Substrates by Conjunctional Freezing-Assisted Ultrasonic Extraction Method", *Proc. IMechE, Part N, J. Nanomater. Nanoeng. Nanosys.*, 232(4) (2018) 135-140.
[25] P. Nyamukamba et al., "Synthetic Methods for Titanium Dioxide Nanoparticles: A Review", Ch. 8, in **"Titanium Dioxide - Material for a Sustainable Environment"**, edited by D. Yang, IntechOpen (2018).
[26] S. Chaiyakun et al., "Growth and characterization of nanostructured anatase phase TiO_2 thin films prepared by DC reactive unbalanced magnetron sputtering", *Appl. Phys. A*, 95(2) (2009) 579-587.
[27] S. Rehman et al., "Strategies of making TiO_2 and ZnO visible light active", *J. Hazard. Mater.*, 170(2-3) (2009) 560-569.
[28] V.H. Castrejón-Sánchez, E. Camps and M. Camacho-López, "Quantification of phase content in TiO_2 thin films by Raman spectroscopy", *Superficies y Vacío*, 27(3) (2014) 88-92.
[29] O.A. Hammadi, F.J. Kadhim and E.A. Al-Oubidy, "Photocatalytic Activity of Nitrogen-Doped Titanium Dioxide Nanostructures Synthesized by DC Reactive Magnetron Sputtering Technique", *Nonl. Opt. Quantum Opt.*, 51(1-2) (2019) 67-78.
[30] X. Chen and S.S. Mao, "Titanium Dioxide Nanomaterials: Synthesis, Properties, Modifications, and Applications", *Chem. Rev.*, 107(7) (2007) 2891-2959.
[31] X. Yue et al., "High surface area, high catalytic activity titanium dioxide aerogels prepared by solvothermal crystallization", *J. Mater. Sci. Technol.*, 47 (2020) 223-230.
[32] Y. Bouachiba et al., "Structural and optical properties of TiO_2 thin films grown by sol-gel dip coating process", *Mater. Sci. Poland*, 32(1) (2014) 1-6.
[33] Z.H. Zaidan, K.H. Mahmood and O.A. Hammadi, "Using Banana Peels for Green Synthesis of Mixed-Phase Titanium Dioxide Nanopowders", *Iraqi J. Appl. Phys.*, 18(4) (2022) 27-30.

 ISSN (print) 2958-8960 (online) xxxx-xxxx Printed in IRAQ